Skeletal Radiology (2021) 50:1637–1646
https://doi.org/10.1007/s00256-021-03718-7

SCIENTIFIC ARTICLE

MRI features of low-grade and high-grade chondrosarcoma in enchondromatosis

Ban Sharif[1] · Ramanan Rajakulasingam[2] · Shahab Sharifi[3] · Paul O'Donnell[2] · Asif Saifuddin[2]

Received: 28 October 2020 / Revised: 4 January 2021 / Accepted: 17 January 2021 / Published online: 23 January 2021

Abstract

Objective To identify magnetic resonance imaging (MRI) features which aid differentiation of low-grade chondral tumours (LGCT-enchondroma and grade 1 chondrosarcoma) from high-grade chondral tumours (HGCT) in patients with enchondromatosis.

Materials and method Approval from our local Research and Innovation Centre of The Institute of Orthopaedics was gained. Patients with enchondromatosis who had biopsy and/or resection of chondral lesions over a 13-year period were identified. The pre-biopsy MRI study was assessed by two experienced musculoskeletal radiologists for tumour origin (intramedullary or surface), cortical expansion, cortical destruction, bone marrow oedema, periosteal reaction, soft tissue mass and soft tissue oedema. MRI features were compared with the final histopathological diagnosis.

Results The study group comprised 25 males and 16 females, with a mean age of 34.9 years (range 6–81 years). Fifty-nine lesions were assessed (12 patients had > 1 tumour treated), including 43 LGCT and 16 HGCT. Significant MRI features suggesting malignant transformation to HGCT for both observers included bone oedema ($p = < 0.001$ and 0.002), periosteal reaction ($p = 0.01$) and soft tissue oedema ($p = 0.001$ and 0.05). Cortical destruction and soft tissue mass were predictors of HGCT in major long bones, but no significant differentiating features were identified in the hands and feet.

Conclusion The presence of bone oedema, periosteal reaction and soft tissue oedema on MRI may indicate a high-grade malignant transformation of chondral tumours in patients with enchondromatosis.

Keywords Enchondromatosis · Ollier disease · Maffucci syndrome · Chondrosarcoma · MRI

Introduction

Enchondromas are common benign chondral tumours which are usually asymptomatic, solitary and almost never progress to secondary chondrosarcoma (CS) [1, 2]. The presence of multiple enchondromas is known as enchondromatosis which has a prevalence of 1:100,000, with Ollier disease (multiple enchondromas) and Maffucci syndrome (multiple enchondromas and soft tissue haemangiomas/lymphangiomas) being the commonest sub-types [2]. The most important complication of enchondromatosis is the malignant transformation to CS for which the reported incidence is highly variable, ranging from 5–50% [3]. Both enchondromas and haemangiomas may become malignant in Maffucci syndrome with a reported risk of 15–56%, compared to 25–30% in Ollier disease [4]. Malignant transformation in both solitary enchondroma and enchondromatosis to CS is intramedullary and preferentially affects long tubular bones such as the femur, humerus and tibia [4, 5]. In addition, multifocal malignant transformation is not uncommon and has been reported in enchondromatosis [2].

The 2020 WHO Classification of Soft Tissue and Bone Tumours [6] differentiates chondral tumours histologically into enchondroma, atypical cartilaginous tumour/grade 1 chondrosarcoma (ACT/Gd1-CS), grade 2 and grade 3 chondrosarcoma (HG-CS) and dedifferentiated chondrosarcoma (DD-CS). Within the setting of enchondromatosis, enchondromas and ACT/Gd1-CS are typically treated with observation or curettage, while HG-CS and

✉ Ban Sharif
ban.sharif@nhs.net

[1] Imaging Department, Northwick Park Hospital, Harrow, England

[2] Imaging Department, Royal National Orthopaedic Hospital, Stanmore, England

[3] Imaging Department, Lister Hospital, Stevenage, England

DD-CS require resection with/without reconstruction. Therefore, clinical and imaging features which aid in the differentiation between enchondroma/ACT/Gd1-CS (hereafter termed low-grade chondral tumours-LGCT) and HG-CS/DD-CS (hereafter termed high-grade chondral tumours-HGCT) would be important. While the differentiation between solitary enchondroma and chondrosarcoma has been extensively studied [7–16], as has the differentiation between solitary ACT/Gd1-CS and HG-CS/DD-CS [17–20], the MRI features differentiating LGCT from HGCT in the setting of enchondromatosis have not been previously reported. The purpose of this study is to identify potential MRI features of chondral lesions which may differentiate LGCT from HGCT in patients with Ollier disease and Maffucci syndrome.

Materials and methods

The study was approved by the local Research and Innovation Centre of The Institute of Orthopaedics under the Integrated Research Application System number 262826, with no requirement for informed patient consent.

A retrospective review of imaging and histopathology reports was undertaken in patients with a known diagnosis of Ollier disease or Maffucci syndrome in the setting of a tertiary referral bone and soft tissue sarcoma service. Inclusion criteria were all patients who had undergone biopsy and/or curettage/resection of chondral lesions over a 13-year period (2007–2020), who had at least one pre-biopsy MRI study of the biopsied or resected lesion. Patients with biopsies of non-chondral lesions and those without an MRI of the index lesion were excluded. Patient age, sex and lesion site were recorded.

Table 1 Skeletal location of 59 chondral lesions

Location	Bone	Intramedullary*	Surface	Total
Long bone ($n = 21$)	Femur	12	0	12
	Humerus	3	1	4
	Tibia	3	0	3
	Fibula	1	0	1
	Radius	1	0	1
Flat bone ($n = 5$)	Ilium	4	0	4
	Acetabulum	1	0	1
Hand ($n = 22$)	Phalanx	18	2	20
	MC	2	0	2
Foot ($n = 11$)	Phalanx	4	1	5
	Medial cuneiform	2	0	2
	Calcaneus	2	0	2
	MT	1	0	1
	Talus	1	0	1
Total		55	4	59

*Based on observer 1 (AS)

A large proportion of the MRI studies were performed at referring hospitals ($n = 21$; 35.6%) resulting in a wide variation of imaging protocols. However, all studies included at least one T1-weighted turbo spin echo (T1W TSE), short tau inversion recovery (STIR) or fat-suppressed T2-weighted fast spin-echo (T2W FSE) sequence, with differing combinations of axial, coronal and sagittal planes. MRI studies performed following referral ($n = 38$: 17 at 1.5T and 21 at 3T; 64.4%) typically consisted of coronal T1W TSE and STIR, sagittal T2W FSE and axial proton density-weighted fast spin echo (PDW FSE) and spectral attenuated inversion recovery (SPAIR) sequences. Contrast enhancement was rarely utilised ($n = 4$; 6.8%) and was therefore not assessed. Retrospective review of pre-biopsy MRI studies was independently performed by two consultant musculoskeletal radiologists with > 26-year (AS) and > 18-year (POD) experience of musculoskeletal tumour imaging. Both reviewers were aware that the patients had enchondromatosis and which chondral tumour had been biopsied, but were blinded to the histopathology results. The specific MRI features assessed included the presence of bone expansion, cortical destruction, peri-lesional bone marrow oedema, periosteal reaction, soft tissue mass and soft tissue oedema according to the following definitions:

- Bone expansion: expansion of the medullary cavity of the bone beyond its expected shape
- Cortical destruction: focal absence of the cortical signal void on any MRI pulse sequence
- Peri-lesional bone marrow oedema: reduced T1W TSE and increase STIR signal intensity (SI) of the bone marrow adjacent to the chondral lesion with poorly defined margins
- Periosteal reaction: fluid SI on fat-suppressed T2W, SPAIR or STIR sequences on the surface of the bone
- Soft tissue mass: direct extension of the intramedullary chondral tumour through the destroyed cortex with the same imaging characteristics of the intramedullary tumour and well-defined peripheral margins
- Soft tissue oedema: poorly defined fluid SI on fat-suppressed T2W, SPAIR or STIR sequences which extended beyond the surface of the bone cortex into the peri-osseous fat or muscles

In addition, the origin of the lesion from bone (intramedullary or surface) was noted. A lesion was defined as intramedullary when it was clearly located within the confines of the cortical signal void and surface when it arose on the outer side of the cortical signal void.

All needle biopsy and surgical histology specimens were reported for clinical purposes by 2 specialist consultant histopathologists in consensus, but were not specifically reviewed

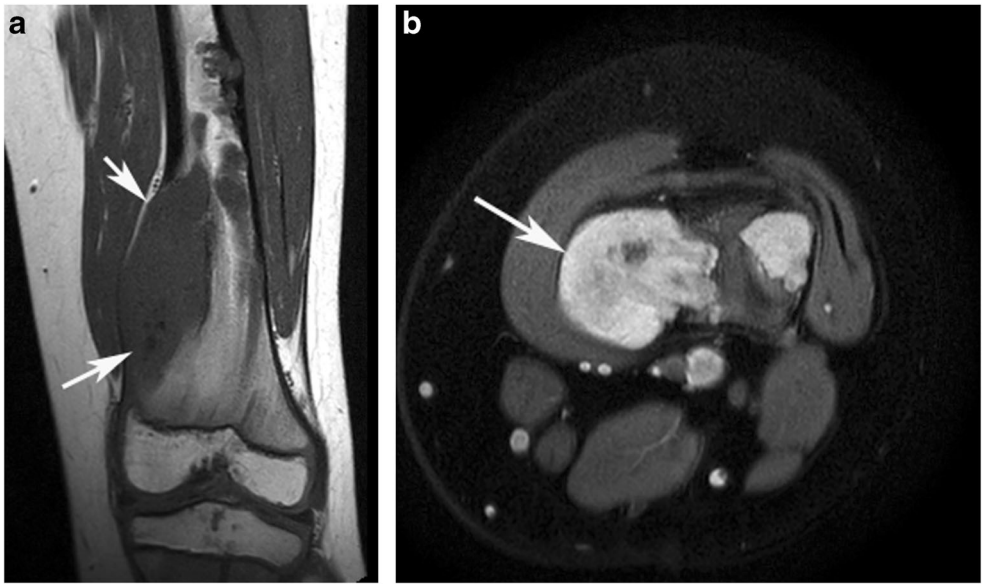

Fig. 1 An 8-year-old boy with Ollier disease and a swollen left distal thigh. **a** Coronal T1W TSE and **b** axial SPAIR MR images show multiple intramedullary chondral tumours with a major lesion expanding the medial femoral metaphysis (arrows). Histologically confirmed LGCT

for the purposes of this study. The histopathology findings were grouped into the following categories: LGCT (enchondroma/ACT/Gd1-CS) and HGCT (grade 2–3 CS or DD-CS). The final histological diagnosis was based on surgical specimens in 48 (81.4%) lesions and needle biopsy in 11 (18.6%).

Statistical analysis

Descriptive statistics were used for patient demographics, skeletal location and final histological diagnosis. The first analysis examined the association between lesion location and final diagnosis (either LGCT or HGCT). The second analysis examined inter-observer agreement for each of the assessed MRI parameters using the kappa statistic. Subsequent analyses examined the relationship between each of the MRI parameters with the final diagnosis (either LGCT or HGCT) for each observer using Fisher's exact test. A further analysis examined the association between lesion location and each of the MRI parameters with the final diagnosis (either LGCT or HGCT) in the location sub-groups, again using Fisher's exact test. These analyses were performed for the long bone and hand/foot sub-groups only since there were an insufficient number of patients in the flat bone sub-group to perform similar analyses. Finally, sensitivity, specificity, positive predictive value (PPV), negative predictive value (NPV) and accuracy of MRI for diagnosing HGCT were calculated.

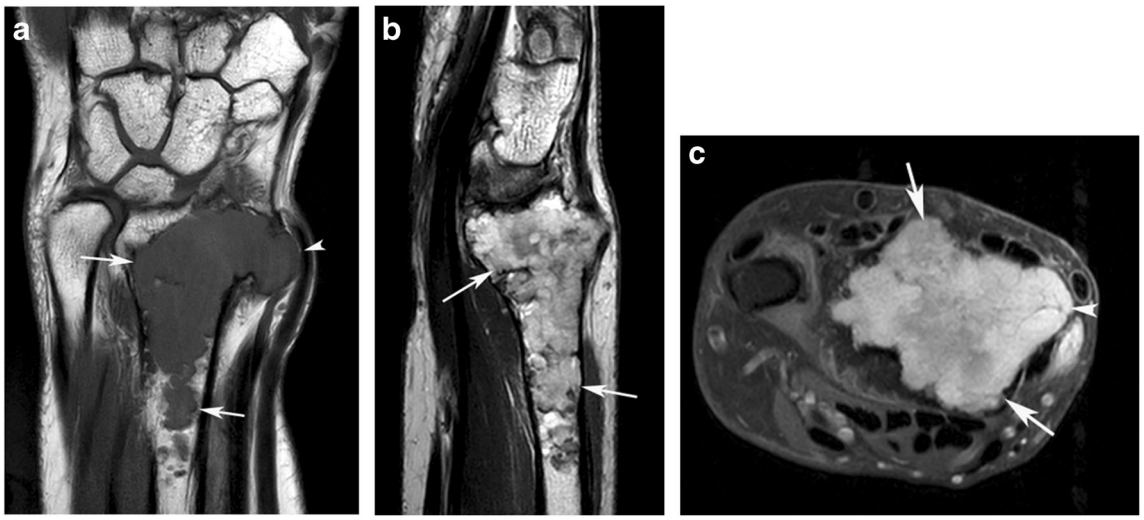

Fig. 2 A 72-year-old female with Ollier disease and a swollen wrist. **a** Coronal T1W TSE, **b** sagittal T2W FSE and **c** axial fat-suppressed T2W FSE MR images show a large distal radial intramedullary chondral tumour (arrows) which has broken through the cortex to form a soft tissue mass (arrowheads **a**, **c**). Histology confirmed a LGCT

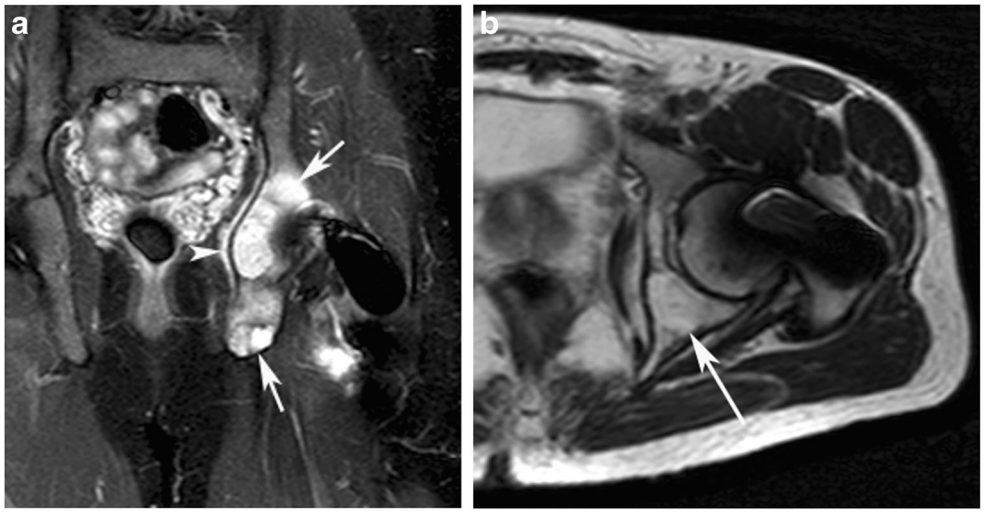

Fig. 3 A 25-year-old male with Ollier disease presenting with left groin pain. **a** Coronal STIR and **b** axial PDW FSE MR images show an extensive chondral tumour in the left acetabulum and ischium (arrows) associated with periosteal reaction (arrowhead **a**). Histology confirmed a HGCT

Results

Forty-one patients fulfilled the inclusion criteria, 25 (61%) males and 16 (39%) females with a mean age at first diagnosis of the index tumour of 34.9 years (range 6–81 years). Twelve patients had more than 1 tumour treated (range 2–4), and therefore, a total of 59 separate lesions were assessed. Thirty-five (85.4%) patients had a diagnosis of Ollier disease and 6 (14.6%) of Maffucci syndrome. Lesion location is presented in Table 1, 21 (35.6%) tumours involving the major long bones (Figs. 1, 2), 5 (8.5%) the flat bones of the pelvis (Fig. 3), 22 (37.3%) the small tubular bones of the hand (Figs. 4, 5) and 11 (18.6%) the tarsal bones or small tubular bones of the feet (Fig. 6). The diagnosis was based on surgical histology in 48 (81.4%) cases (curettage in 23, resection in 19 and amputation in 6) and by needle biopsy alone in 11 (18.6%) cases. Final histology revealed 43 LGCT and 16 HGCT. Of the latter, 12 occurred in Ollier disease and 4 in Maffucci syndrome. Table 2 presents the relationship between lesion location and final histology which suggested a significant association, the occurrence of a HGCT being highest in the flat bones (80%) and lowest in the hand/foot (13%) (p = 0.004).

Inter-observer agreement for the assessed MRI variables is presented in Table 3, which showed that strength of agreement typically varied between 0.4 and 0.6 suggesting moderate agreement, but a good agreement for bone and soft tissue oedema (both > 0.6). Tables 4 and 5 present the relationship between assessed MRI variables and final histology for each observer. The results for both observers suggested significant associations with HGCT for bone oedema, periosteal reaction and soft tissue oedema, but for the 2nd observer (POD), the result for soft tissue oedema was only of borderline statistical significance. The relationship between MRI variables and final histology for major long bone lesions indicated that

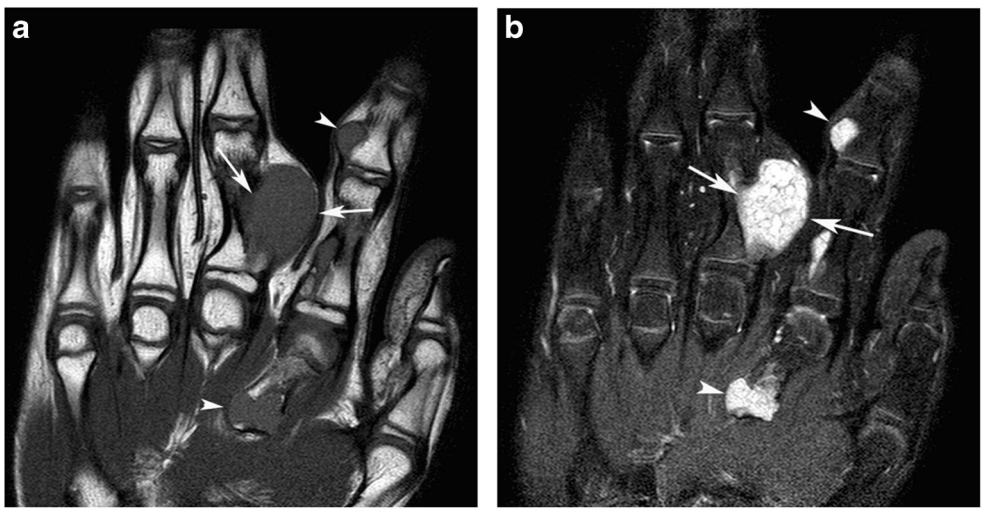

Fig. 4 A 12-year-old boy with Ollier disease presenting with a large swelling of the middle finger proximal phalanx. **a** Coronal T1W TSE and **b** STIR MR images show a large chondral tumour arising from the radial side of the middle finger proximal phalanx (arrows) with several smaller lesions demonstrated (arrowheads). The major lesion was a histologically proven LGCT

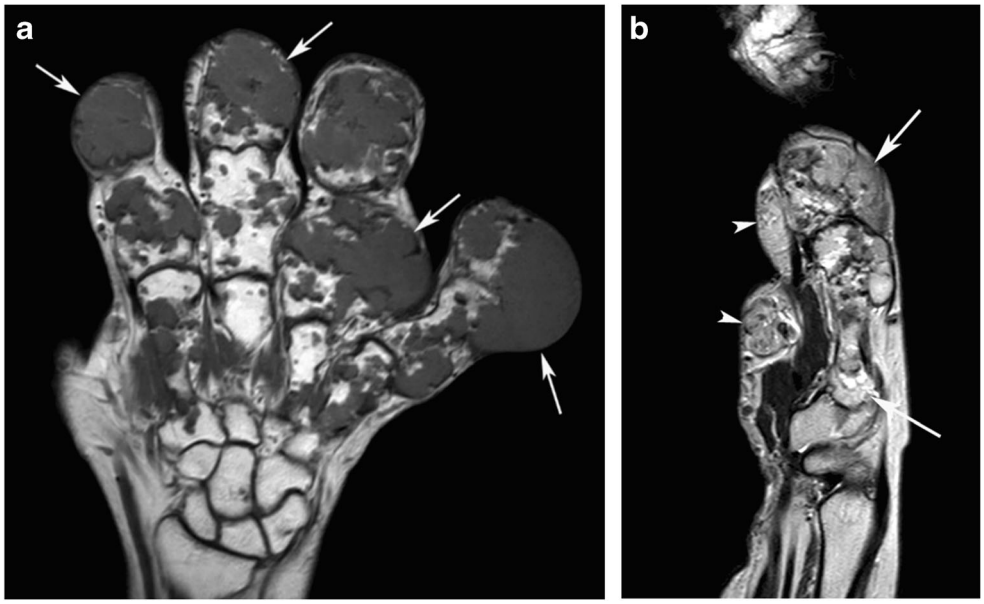

Fig. 5 A 25-year-old male with Maffucci syndrome presenting with multiple swollen fingers. **a** Coronal T1W TSE and **b** sagittal T2W FSE MR images show multiple chondral tumours expanding the fingers (arrows) associated with soft tissue haemangiomas (arrowheads **b**). Histology confirmed HGCT arising from the little finger

cortical destruction and bone oedema were significant indicators of HGCT for observer 1 (AS) and that cortical destruction, periosteal reaction and soft tissue mass were predictors of HGCT for observer 2 (POD) (Figs. 7, 8, 9). However, there were no individual MRI predictors of HGCT for either observer in the small bones of the hands and feet (Fig. 10).

Table 6 presents the sensitivity, specificity, PPV, NPV and accuracy of each of the assessed MRI variables for a diagnosis of HGCT for each observer. The most sensitive indicators of HGCT were intramedullary location and cortical expansion, while the most specific were bone oedema, periosteal reaction and soft tissue oedema. These were also the most accurate for a diagnosis of HGCT.

Discussion

The current study aimed to determine MRI features which may be indicative of high-grade chondrosarcomatous transformation in patients with enchondromatosis. For the overall population, the presence of bone oedema, periosteal reaction and soft tissue oedema was highly suggestive of HGCT, while for major long bone tumours, cortical destruction and soft tissue mass were also relevant features. No MRI features were predictive of HGCT in the small bones.

Previous studies have identified a peak age of > 40 years and a predilection for the pelvis and long tubular bones as differentiating features of chondrosarcoma in the setting of

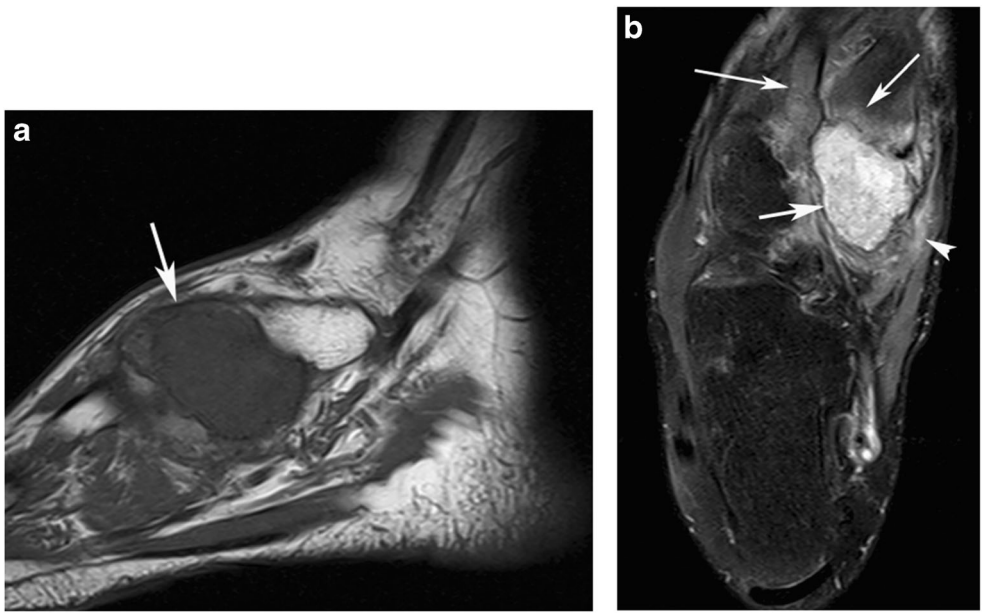

Fig. 6 A 38-year-old male with Ollier disease presenting with medial midfoot pain. **a** Sagittal T1W TSE and **b** axial fat-suppressed T2W FSE MR images show a chondral lesion expanding the medial cuneiform (arrows) associated with both bone marrow (thin arrows **b**) and soft tissue (arrowhead **b**) oedema. Histologically confirmed a HGCT

Table 2 Association between lesion location and final diagnosis

Variable	Category	LGCT *n* (%)	HGCT *n* (%)	*P* value
Lesion location	Long bone	14 (64)	8 (36)	0.004
	Flat bone	1 (20)	4 (80)	
	Hand/foot	28 (87)	4 (13)	

enchondromatosis [2, 3, 7, 21]. The current study demonstrates that the majority of HGCT occurred in long bone locations and that 80% of pelvic tumours were HGCT, while 87% of small bone lesions of the hands and feet were LGCT. Although the malignant transformation of benign solitary enchondroma in the hands and feet to secondary CS is extremely rare, it has been described in the presence of enchondromatosis [3, 22, 23], but less frequently in the hands and feet than in major long and flat bones. We did not assess patient age since 12 patients had further tumours at various times during their disease course, ranging from 0–9 years following presentation with the index lesion.

The risk of malignant transformation is higher in Maffucci syndrome than in Ollier disease [4], which is supported by our results where 4 of 6 (66.7%) patients with Maffucci syndrome developed a HGCT compared to only 10 of 35 (28.6%) patients with Ollier disease (2 patients having 2 tumours each). This is similar to the findings of Verdegaal et al. who described 66 CS in 161 patients with Ollier disease or Maffucci syndrome, 57 of 144 (39.6%) in Ollier disease and 9 of 17 (53%) in Maffucci syndrome [3]. However, comparison with our results is difficult since Verdegaal's study included ACT/grade 1 CS within the CS group, which accounted for 52% of cases [3].

Previously reported radiographic features suggestive of the development of chondrosarcoma in enchondromatosis include cortical destruction and extra-osseous soft tissue mass [3]. Several studies have assessed the MRI features which may

Table 3 Summary of MRI parameters and inter-observer agreement

Variable	Category	Observer 1 *n* (%)	Observer 2 *n* (%)	Kappa (95% CI)
Site in bone	Intramedullary	55 (93)	48 (81)	0.48 (0.26, 0.70)
	Surface	4 (7)	11 (19)	
Bone expansion	No	8 (14)	23 (39)	0.39 (0.19, 0.60)
	Yes	51 (86)	36 (61)	
Cortical destruction	No	20 (34)	29 (49)	0.56 (0.31, 0.80)
	Yes	39 (66)	30 (51)	
Bone marrow oedema	No	42 (71)	38 (64)	0.77 (0.51, 1.00)
	Yes	17 (29)	21 (36)	
Periosteal reaction	No	52 (88)	52 (88)	0.51 (0.26, 0.77)
	Yes	7 (12)	7 (12)	
Soft tissue mass	No	18 (31)	28 (47)	0.52 (0.28, 0.76)
	Yes	41 (69)	31 (53)	
Soft tissue oedema	No	42 (71)	48 (81)	0.63 (0.39, 0.88)
	Yes	17 (29)	11 (19)	

Table 4 Univariate associations between MRI parameters and final diagnosis for observer 1 (AS)

Variable	Category	LGCT *n* (%)	HGCT *n* (%)	*P* value
Site in bone	Intramedullary	39 (71)	16 (29)	0.57
	Surface	4 (100)	0 (0)	
Bone expansion	No	6 (75)	2 (25)	1.00
	Yes	37 (73)	14 (27)	
Cortical destruction	No	15 (75)	5 (25)	1.00
	Yes	28 (72)	11 (28)	
Bone marrow oedema	No	37 (88)	5 (12)	<0.001
	Yes	6 (35)	11 (65)	
Periosteal reaction	No	41 (79)	11 (21)	0.01
	Yes	2 (29)	5 (71)	
Soft tissue mass	No	13 (72)	5 (28)	1.00
	Yes	30 (73)	11 (27)	
Soft tissue oedema	No	36 (86)	6 (14)	0.001
	Yes	7 (41)	10 (59)	

Table 5 Univariate associations between MRI parameters and final diagnosis for observer 2 (POD)

Variable	Category	LGCT *n* (%)	HGCT *n* (%)	*P* value
Site in bone	Intramedullary	33 (69)	15 (31)	0.26
	Surface	10 (91)	1 (9)	
Bone expansion	No	19 (83)	4 (17)	0.24
	Yes	24 (67)	12 (33)	
Cortical destruction	No	23 (79)	6 (21)	0.38
	Yes	20 (67)	10 (33)	
Bone marrow oedema	No	33 (87)	5 (13)	0.002
	Yes	10 (48)	11 (52)	
Periosteal reaction	No	41 (79)	11 (21)	0.01
	Yes	2 (29)	5 (71)	
Soft tissue mass	No	23 (82)	5 (18)	0.15
	Yes	20 (65)	11 (35)	
Soft tissue oedema	No	38 (79)	10 (21)	0.05
	Yes	5 (45)	6 (55)	

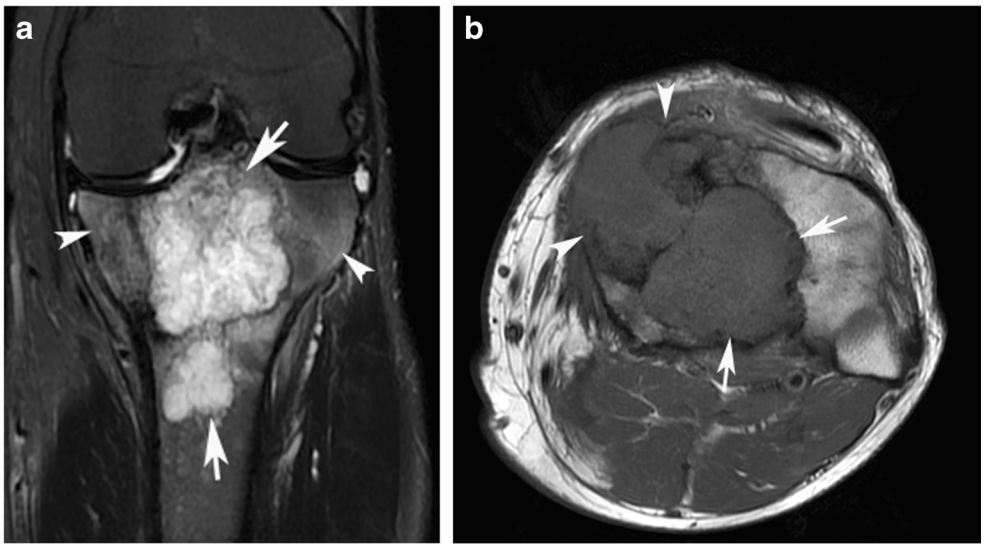

Fig. 7 A 64-year-old male with Ollier disease presenting with a painful swelling on the anteromedial proximal calf. **a** Coronal STIR and **b** axial T1W TSE MR images show a chondral lesion in the central proximal tibia (arrows) with associated bone marrow oedema (arrowheads **a**) and an anterior extra-osseous soft tissue mass extending through the destroyed tibial cortex (arrowheads **b**). Histologically confirmed HGCT

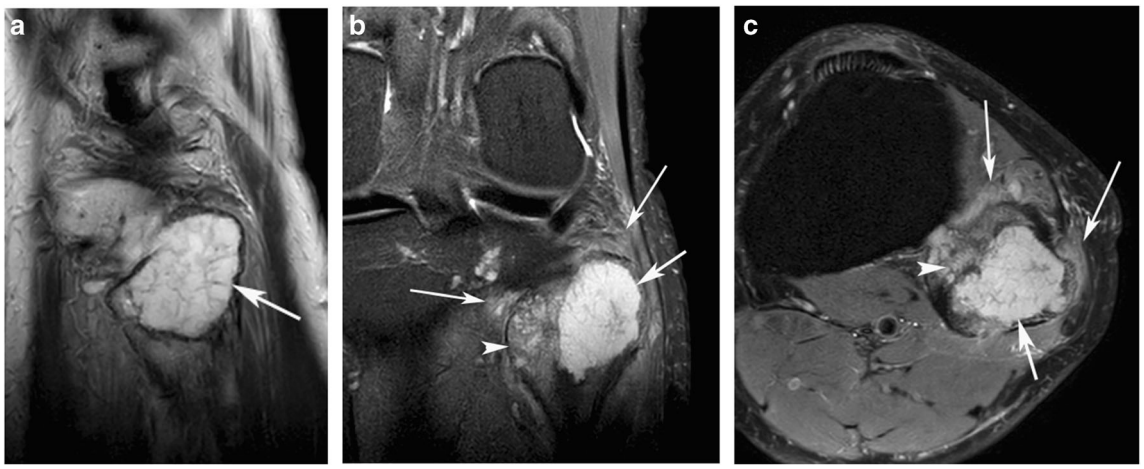

Fig. 8 A 25-year-old male with Ollier disease and swelling over the lateral left knee. **a** Sagittal PDW FSE, **b** coronal STIR and **c** axial SPAIR MR images show an intramedullary chondral tumour in the fibular head (arrows) which has broken through the cortex to form a small soft tissue mass with associated bone marrow (arrowheads **b**, **c**) and soft tissue (thin arrows **b**, **c**) oedema. Histology confirmed a HGCT

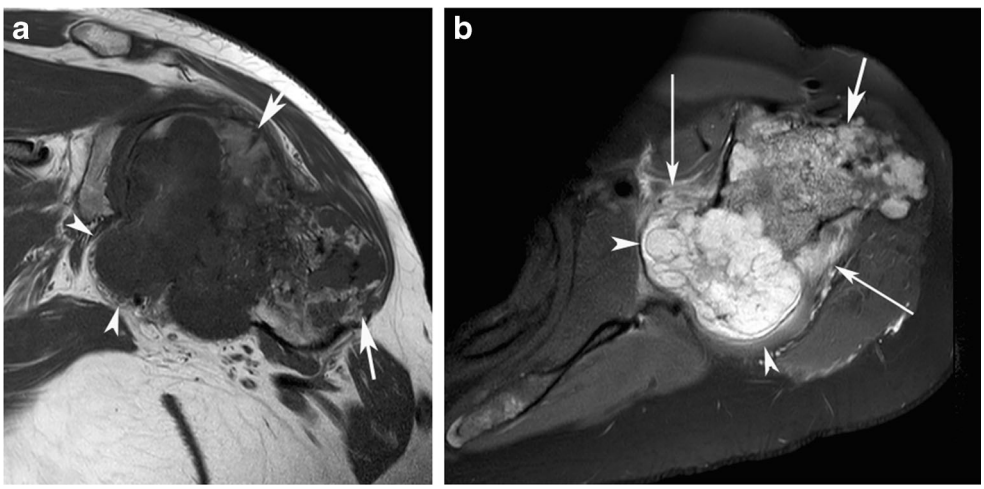

Fig. 9 A 26-year-old male with Ollier disease presenting with left shoulder pain. **a** Coronal T1W TSE and **b** axial SPAIR MR images show expansion and deformity of the proximal humerus which contains multiple chondral tumours (arrows), and also a particularly large tumour mass extending through the medial metaphyseal cortex (arrowheads) with associated soft tissue oedema (thin arrows **b**). Histology confirmed a HGCT

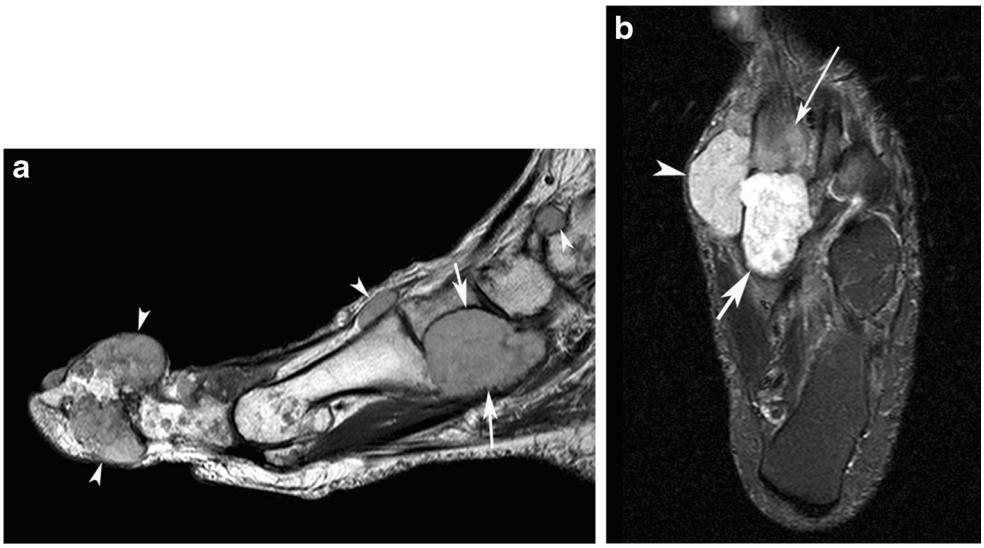

Fig. 10 A 64-year-old male with Ollier disease presenting with a swelling on the medial midfoot. **a** Sagittal T1W TSE and **b** axial SPAIR MR images show a chondral lesion in the medial cuneiform (arrows) with multiple further smaller chondral lesions (arrowheads **a**) and associated bone marrow oedema (thin arrow **b**). A prominent soft tissue mass is also noted adjacent to the medial cuneiform (arrowhead **b**). Biopsy of the soft tissue mass confirmed a LGCT

differentiate between LGCT and HGCT in the setting of a solitary lesion [17–19], which were summarised in a systematic review by Deckers et al. who concluded that loss of entrapped fatty marrow, cortical breakthrough and extra-

Table 6 Diagnostic performance of MRI variables for the prediction of HGCT for both observers

MRI feature	Statistic	Observer 1		Observer 2	
		n/*N*	% (95% CI)	*n*/*N*	% (95% CI)
Intramedullary location	Sensitivity	16/16	100% (79%, 100%)	15/16	94% (70%, 100%)
	Specificity	4/43	9% (3%, 22%)	10/43	23% (12%, 39%)
	Positive PV	16/55	29% (18%, 43%)	15/48	31% (19%, 46%)
	Negative PV	4/4	100% (40%, 100%)	10/11	91% (59%, 100%)
	Accuracy	20/59	34% (22%, 47%)	25/59	42% (30%, 56%)
Bone expansion	Sensitivity	14/16	88% (62%, 98%)	12/16	75% (48%, 93%)
	Specificity	6/43	14% (5%, 28%)	19/43	44% (29%, 60%)
	Positive PV	14/51	28% (16%, 42%)	12/36	33% (19%, 51%)
	Negative PV	6/8	75% (35%, 97%)	19/23	83% (61%, 95%)
	Accuracy	20/59	34% (22%, 47%)	31/59	53% (39%, 66%)
Cortical destruction	Sensitivity	11/16	69% (41%, 89%)	10/16	63% (35%, 85%)
	Specificity	15/43	35% (21%, 51%)	23/43	54% (38%, 69%)
	Positive PV	11/39	28% (15%, 45%)	10/30	33% (17%, 53%)
	Negative PV	15/20	75% (51%, 91%)	23/29	79% (60%, 92%)
	Accuracy	28/59	44% (31%, 58%)	33/59	56% (42%, 69%)
Bone marrow oedema	Sensitivity	11/16	69% (41%, 89%)	11/16	69% (41%, 89%)
	Specificity	37/43	86% (72%, 95%)	33/43	77% (61%, 88%)
	Positive PV	11/17	65% (38%, 86%)	11/21	52% (30%, 74%)
	Negative PV	37/42	88% (74%, 96%)	33/38	87% (72%, 96%)
	Accuracy	48/59	81% (69%, 90%)	44/59	75% (62%, 85%)
Periosteal reaction	Sensitivity	5/16	31% (11%, 59%)	5/16	31% (11%, 59%)
	Specificity	41/43	95% (84%, 99%)	41/43	95% (84%, 99%)
	Positive PV	5/7	71% (29%, 96%)	5/7	71% (29%, 96%)
	Negative PV	41/52	79% (65%, 89%)	41/52	79% (65%, 89%)
	Accuracy	46/59	78% (65%, 88%)	46/59	78% (65%, 88%)
Soft tissue mass	Sensitivity	11/16	69% (41%, 89%)	11/16	69% (41%, 89%)
	Specificity	13/43	30% (17%, 46%)	23/43	54% (38%, 69%)
	Positive PV	11/41	27% (14%, 43%)	11/31	36% (19%, 55%)
	Negative PV	13/18	72% (47%, 90%)	23/28	82% (63%, 94%)
	Accuracy	24/59	41% (28%, 54%)	34/59	58% (44%, 70%)
Soft tissue oedema	Sensitivity	10/16	63% (35%, 85%)	6/16	38% (15%, 65%)
	Specificity	36/43	84% (69%, 93%)	38/43	88% (75%, 96%)
	Positive PV	10/17	59% (33%, 82%)	6/11	55% (23%, 17%)
	Negative PV	36/42	86% (72%, 95%)	38/48	79% (65%, 90%)
	Accuracy	46/59	78% (65%, 88%)	42/59	75% (62%, 85%)

osseous soft tissue extension was more often seen with HGCT than LGCT [20]. These studies predominantly assessed major long bone lesions, with no study currently published looking at the MRI differentiation of LGCT from HGCT in a large group of tumours arising from flat bones. Douis et al. [18] found that bone oedema, periosteal reaction, bone expansion, cortical destruction, soft tissue mass and soft tissue oedema were all features associated with HGCT in the major long bones. All of these features apart from bone expansion were also found to favour HGCT of the major long bones in patients with enchondromatosis. Fayed et al. [11] and Ogose et al. [14] found that chondrosarcomas of the hands and feet had associated extra-osseous soft tissue mass in 70% and 79% of cases respectively, while Zhou et al. found bone expansion to be indicative of secondary CS in enchondromatosis of the hands and feet [24]. However, in the current study, there were no MRI features which helped to differentiate LGCT and HGCT in the hands and feet.

The current study has several limitations, including its retrospective nature and a relatively small sample size. In 11 cases, histological diagnosis relied purely on needle biopsy which may underestimate the grade of chondral tumours compared to surgical histology [25]. In most cases, there was no previous MRI study of the biopsied lesion for assessment of lesion growth as a further indication of tumour grade. The majority of MRI examinations were performed prior to referral with differing protocols, which may have affected the appearances of peri-lesional bone marrow and soft tissue oedema from case to case. Only a minority of contrast-enhanced studies were available, but as the aim of the study was to evaluate whether MRI could differentiate low- and high-grade chondrosarcoma, techniques such as dynamic contrast-enhanced MRI and diffusion-weighted imaging (DWI) were not assessed. The former has not been shown to be of value in differentiating enchondroma from chondrosarcoma [13], while DWI has also not been found useful for the identification of chondrosarcoma [26]. Finally, FDG-PET studies were also not available in any cases. FDG-PET has shown value in differentiating low-grade chondral tumours from higher-grade lesions based on SUVmax [27], and therefore, this could be the subject of further research in the setting of enchondromatosis.

In conclusion, the current study suggests that high-grade CS is more likely to occur in Maffucci syndrome and in tumours arising from the pelvis. The presence of bone oedema, periosteal reaction and soft tissue oedema on MRI may indicate high-grade malignant transformation in patients with enchondromatosis. In addition, cortical destruction and soft tissue mass are features suggestive of HGCT in major long bone lesions, but no significant differentiating features were identified in the small bones of the hands and feet.

Compliance with ethical standards

Conflict of interest The authors declare no conflict of interest.

References

1. Pansuriya TC, Kroon HM, Bovée JVMG. Enchondromatosis: insights on the different subtypes. Int J Clin Exp Pathol. 2010 Jun 26;3(6):557–69.
2. Herget GW, Strohm P, Rottenburger C, Kontny U, Krauß T, Bohm J, et al. Insights into Enchondroma, Enchondromatosis and the risk of secondary Chondrosarcoma. Review of the literature with an emphasis on the clinical behaviour, radiology, malignant transformation and the follow up. Neoplasma. 2014;61(4):365–78.
3. Verdegaal SHM, Bovée JVMG, Pansuriya TC, Grimer RJ, Ozger H, Jutte PC, et al. Incidence, predictive factors, and prognosis of chondrosarcoma in patients with Ollier disease and Maffucci syndrome: an international multicenter study of 161 patients. The Oncologist. 2011 Dec;16(12):1771–9.
4. Zwenneke Flach H, Ginai AZ, Wolter OJ. Best cases from the AFIP: Maffucci syndrome: radiologic and pathologic findings. RadioGraphics. 2001 Sep;21(5):1311–6.
5. Douis H, Saifuddin A. The imaging of cartilaginous bone tumours. II. Chondrosarcoma. Skeletal Radiol. 2013 May;42(5):611–26.
6. WHO, Classification of Tumours Editorial Board. Soft tissue and bone tumours. 2020.
7. Choi B-B, Jee W-H, Sunwoo H-J, Cho J-H, Kim J-Y, Chun K-A, et al. MR differentiation of low-grade chondrosarcoma from enchondroma. Clin Imaging. 2013 May;37(3):542–7.
8. Murphey MD, Flemming DJ, Boyea SR, Bojescul JA, Sweet DE, Temple HT. Enchondroma versus chondrosarcoma in the appendicular skeleton: differentiating features. RadioGraphics. 1998 Sep;18(5):1213–37.
9. Geirnaerdt MJ, Hermans J, Bloem JL, Kroon HM, Pope TL, Taminiau AH, et al. Usefulness of radiography in differentiating enchondroma from central grade 1 chondrosarcoma. Am J Roentgenol. 1997 Oct;169(4):1097–104.
10. Vanel D, Kreshak J, Larousserie F, Alberghini M, Mirra J, De Paolis M, et al. Enchondroma vs. chondrosarcoma: a simple, easy-to-use, new magnetic resonance sign. Eur J Radiol. 2013 Dec;82(12):2154–60.
11. Fayad LM, Ahlawat S, Khan MS, McCarthy E. Chondrosarcomas of the hands and feet: a case series and systematic review of the literature. Eur J Radiol. 2015 Oct;84(10):2004–12.
12. Crim J, Schmidt R, Layfield L, Hanrahan C, Manaster BJ. Can imaging criteria distinguish enchondroma from grade 1 chondrosarcoma? Eur J Radiol. 2015 Nov;84(11):2222–30.
13. Douis H, Parry M, Vaiyapuri S, Davies AM. What are the differentiating clinical and MRI-features of enchondromas from low-grade chondrosarcomas? Eur Radiol. 2018 Jan;28(1):398–409.
14. Ogose A, Unni KK, Swee RG, May GK, Rowland CM, Sim FH. Chondrosarcoma of small bones of the hands and feet. Cancer. 1997 Jul 1;80(1):50–9.
15. De Coninck T, Jans L, Sys G, Huysse W, Verstraeten T, Forsyth R, et al. Dynamic contrast-enhanced MR imaging for differentiation between enchondroma and chondrosarcoma. Eur Radiol. 2013 Nov;23(11):3140–52.
16. De Beuckeleer LHL, De Schepper AMA, Ramon F, Somville J. Magnetic resonance imaging of cartilaginous tumors: a retrospective study of 79 patients. Eur J Radiol. 1995 Nov;21(1):34–40.

17. Yoo HJ, Hong SH, Choi J-Y, Moon KC, Kim H-S, Choi J-A, et al. Differentiating high-grade from low-grade chondrosarcoma with MR imaging. Eur Radiol. 2009 Dec;19(12):3008–14.
18. Douis H, Singh L, Saifuddin A. MRI differentiation of low-grade from high-grade appendicular chondrosarcoma. Eur Radiol. 2014 Jan;24(1):232–40.
19. Fritz B, Müller DA, Sutter R, Wurnig MC, Wagner MW, Pfirrmann CWA, et al. Magnetic resonance imaging–based grading of cartilaginous bone tumors: added value of quantitative texture analysis. Invest Radiol. 2018 Nov;53(11):663–672.
20. Deckers C, Steyvers MJ, Hannink G, Schreuder HWB, de Rooy JWJ, Van Der Geest ICM. Can MRI differentiate between atypical cartilaginous tumors and high-grade chondrosarcoma? A systematic review. Acta Orthop. 2020 Jul 3;91(4):471–8.
21. Vázquez-García B, Valverde M, San-Julián M. [Ollier disease: benign tumours with risk of malignant transformation. A review of 17 cases]. An Pediatr Barc Spain 2003. 2011 Mar;74(3):168–73.
22. Brien EW, Mirra JM, Kerr R. Benign and malignant cartilage tumors of bone and joint: their anatomic and theoretical basis with an emphasis on radiology, pathology and clinical biology. Skeletal Radiol. 1997 Jun 9;26(6):325–53.
23. Sun TC, Swee RG, Shives TC, Unni KK. Chondrosarcoma in Maffucci's syndrome. J Bone Joint Surg Am. 1985 Oct;67(8):1214–9.
24. Zhou J, Jiang Z-M, Zhang H-Z, Huang J. Clinicopathologic study of Ollier's disease and its chondrosarcomatous transformation. Zhonghua Bing Li Xue Za Zhi. 2009 Oct;38(10):673–7.
25. Oliveira I, Chavda A, Rajakulasingam R, Saifuddin A. Chondral tumours: discrepancy rate between needle biopsy and surgical histology. Skeletal Radiol [Internet]. 2020 Mar 9 [cited 2020 May 13]; Available from: http://link.springer.com/10.1007/s00256-020-03406-y
26. Douis H, Jeys L, Grimer R, Vaiyapuri S, Davies AM. Is there a role for diffusion-weighted MRI (DWI) in the diagnosis of central cartilage tumors? Skeletal Radiol. 2015 Jul;44(7):963–9.
27. Subhawong TK, Winn A, Shemesh SS, Pretell-Mazzini J. F-18 FDG PET differentiation of benign from malignant chondroid neoplasms: a systematic review of the literature. Skeletal Radiol. 2017 Sep;46(9):1233–9.